

11463
42
c.1

NACA

RESEARCH MEMORANDUM

FLIGHT INVESTIGATION OF THE JETTISONABLE-NOSE METHOD
OF PILOT ESCAPE USING ROCKET-PROPELLED MODELS

By

Reginald R. Lundstrom and Burke R. O'Kelly

Langley Aeronautical Laboratory
Langley Air Force Base, Va.

CLASSIFICATION CANCELLED

CLASSIFIED DO Authority *NACA R7-2-4-32* Date *8/18/54*

This document contains classified information affecting the National Defense of the United States within the meaning of the Espionage Act, USC 50:81 and 82. Its transmission or revelation of its contents in any manner to an unauthorized person is prohibited by law. Information so classified may be imparted only to persons in the military and naval services of the United States, to official civilian officers and employees of the Federal Government who have a legitimate interest therein, and to United States citizens of known loyalty and discretion who of necessity must be informed thereof.

8/31/54 See

NATIONAL ADVISORY COMMITTEE
FOR AERONAUTICS
WASHINGTON

June 2, 1949

UNCLASSIFIED



UNCLASSIFIED

NATIONAL ADVISORY COMMITTEE FOR AERONAUTICS

RESEARCH MEMORANDUM

FLIGHT INVESTIGATION OF THE JETTISONABLE-NOSE METHOD
OF PILOT ESCAPE USING ROCKET-PROPELLED MODELS

By Reginald R. Lundstrom and Burke R. O'Kelly

SUMMARY

Two rocket-propelled models to test the jettisonable-nose method of pilot escape were launched by the Langley Laboratory. During the flight of the first model the nose came off during power-on flight due to the malfunction of a release latch and was damaged by collision with a wing of the main body. The nose section of the second model was jettisoned successfully at the end of its power-on flight at a Mach number of 0.87. Accelerations produced were well within human tolerance. The drag-weight ratios of nose and rear bodies were such that the deceleration of the nose was less than that of the rear body. The shielding effect of the nose on the rear body during separation was appreciable and forcible separation appears necessary.

INTRODUCTION

As the speeds of piloted aircraft advance into the transonic and supersonic ranges, conventional means of pilot escape in cases of emergency appear to be inadequate. Ejection seats of the type mentioned in reference 1 should make escape much easier at subsonic speeds, but, in their present form, their use for escape at speeds in excess of 550 miles per hour at moderately low altitudes does not appear practical.

The human body is quite sensitive to accelerations and in any escape device the accelerations should be kept at a minimum for the safety and comfort of the pilot. Reference 2 lists the physiological effects of acceleration. Because high-speed airplanes are expected to travel at high altitudes, the escape method must provide the pilot with oxygen until a low altitude has been reached.

One method of escape which appears practical is to jettison the complete nose section of the airplane and, after it has been decelerated to a fairly low-subsonic speed, have the pilot leave the nose section with his own personal parachute. Reference 3 and recent unpublished low-speed

UNCLASSIFIED

data indicate that some means will be necessary to stabilize such a jettisoned nose section to prevent linear and centripetal accelerations dangerous to the pilot and show that the addition of suitable fins would accomplish this at low speeds. Rocket-propelled test vehicles designated RM-11A and RM-11B have been constructed and tested to investigate the problems of jettisoning such a fin-stabilized nose section during high-speed power-off flight and to measure the accelerations throughout its flight path. The results of the tests of these two vehicles are covered by the present paper. The nose-section model used was not a model of any particular airplane nose but was fairly representative of a $\frac{1}{4}$ - or $\frac{1}{5}$ -scale airplane nose section dynamically similar at about 40,000 feet altitude. Since one of the problems of this escape method is to insure that the rear body will not overtake the jettisoned nose, an attempt was made to measure the relative decelerations of the two sections. The models were launched at the Pilotless Aircraft Research Station, Wallops Island, Va.

APPARATUS AND METHODS

Model

The RM-11 rocket-propelled test vehicle covered by the present paper was similar to the FR-1-A (reference 4) and so constructed that the nose could be jettisoned at a station 40.5 inches from its tip. The nose section had four stabilizing fins of 32.4-square-inches area each, permanently installed such that the trailing edge was at the separation station and the center of gravity was located 60 percent back of the nose. The results of previous tests of a one-half-scale model of this nose configuration in the Langley 20-foot free-spinning tunnel (reference 3) had indicated that the fin size selected for this center-of-gravity location would give good stability. The center-of-gravity position of the jettisonable nose was made approximately 60 percent back from the tip because designers of jettisonable nose sections for most research airplanes have found that no practical layout will give a center-of-gravity location farther forward. The rear body was designed so that it would be stable after separation. A sketch of the model is shown in figure 1 and a photograph in figure 2. The mass-balance characteristics of the two models used are listed in table I. The model was launched from a near zero length launcher at an angle of 60° using methods described in reference 4.

A sketch of the jettison mechanism is shown in figure 3. A mercury deceleration switch was used to close the firing circuit of the jettison charge and a delay squib of approximately 0.8 second was used to insure complete loss of thrust before ejection. When the jettison charge is fired, the piston cannot move; the jettison cylinder therefore moves forward on the piston, releasing the toggle latches. The cylinder continues to move forward off the piston, carrying the entire nose section with it.

Because it was felt that the failure of a release latch in the first test (model A) was due to high bearing forces and/or a twisting moment during power-on flight, bearing plates as shown in figure 4 were installed in model B to absorb these forces and moments so that they would not be applied on the ejection mechanism.

The nose section was equipped with drag flaps which were driven radially outward by a small electric motor. The flaps started to open approximately 2 seconds after ejection and were completely out 6 seconds after ejection. The flaps are shown retracted and opened in figures 5 and 6, respectively.

Instrumentation

A four-channel telemeter was installed in the nose section to transmit signals from four accelerometers. Three accelerometers to measure longitudinal (along X-axis), transverse (along Y-axis), and normal (along Z-axis of the nose section) accelerations were installed in the jettisonable nose at the locations given in table II. A longitudinal accelerometer installed in the rear body was connected to the telemeter in the nose section by a pull-out plug and about 15 feet of excess cable in order that readings of relative acceleration between the two bodies could be obtained during separation.

A continuous-wave Doppler radar was used to record velocity and an SCR-584 pulse-type radar was used to record trajectory of the models. Atmospheric conditions prevailing at the time of flight were obtained by a radiosonde.

RESULTS

Model A

The nose section of model A came off prematurely after 4.65 seconds of power-on flight (velocity 615 ft per sec; Mach number 0.54) due to the malfunction of a release latch. The nose yawed to the right, became detached from the rear body, and was struck by the right wing. One nose fin was torn off but the telemeter remained in operation and a record was obtained. Directly after the nose came off, peak accelerations of approximately $\pm 12g$ occurred about various axes due to contact and interference with the rear body. Two seconds later these oscillations became more or less regular and had peak values of about $1g$ to $-7g$. The telemeter record indicates that the nose section was assuming a helical flight path. A plot of accelerations against time from 7 seconds after launching is shown in figure 7. Since the nose was not forcibly ejected, the automatic switch to the motor which operates the flaps was not turned on.

Model B

Model B was launched smoothly and good telemeter signals were received. Rocket thrust decreased after 8.4 seconds of flight and deceleration of the model started at 8.6 seconds. The nose was jettisoned at 9.86 seconds ($M = 0.87$) producing an instantaneous forward acceleration on the nose section of 10.8g and instantaneous transverse and normal accelerations of 2.4g and 0.75g, respectively. After ejection, the drag of the nose section produced a longitudinal deceleration of about 3.25g (maximum), gradually decreasing as the speed decreased. The normal and transverse accelerations after separation were limited to small oscillations of 0g to 1.3g maximum. A plot of accelerations against time during ejection is shown in figure 8.

Readings of the accelerometer in the rear section were obtained for about 0.3 second after separation, making it possible to calculate the drag of the rear body until it was about 5.5 feet behind the nose section. A plot of the longitudinal accelerations of the nose and rear sections immediately following ejection is shown in figure 9. The accelerometer traces are rough because the nose was oscillating. A plot of drag coefficient C_D against separation distance is shown in figure 10. These drag coefficients are based on body cross-section area at the separation station. Since both bodies were free, there is no assurance that the nose was not displaced somewhat laterally or normally from the rear body as they separated.

The continuous-wave Doppler radar gave a record of the velocities of both sections up to 14.72 seconds. This is presented as a velocity-time plot in figure 11, and separation velocity-time plot in figure 12.

A plot of flight time against altitude as obtained from the pulse-type tracking radar is shown in figure 13. The pulse-type radar read the rear-body position from separation until 25 seconds after launching, both sections from 25 to 26 seconds after launching, and thereafter only the nose section. Some intermediate values were obtained by integrating the velocity-time curve plot of the continuous-wave Doppler record. Also included in figure 13 are the atmospheric conditions at time of flight as recorded by the radiosonde.

While there was no instrumentation to record operation of the flap motor, reduction of the drag data to a plot of drag coefficient against velocity (fig. 14) indicates that they operated, but in an irregular manner. An integration of the accelerometer record indicates that the terminal velocity was approximately 500 feet per second at sea level.

DISCUSSION

The flights of RM-11 models indicate that the nose section should be jettisoned after the thrust has been cut off. This might not be difficult to do by having the escape device also cut off the fuel supply, but the time lag between fuel cut-off and complete loss of thrust is very important. Even if the design were such that the rear body became unstable after jettisoning the nose, because of the short distance of forcible separation, the shielding effect of the nose on the rear body, and the large moment of inertia of the rear body, it seems improbable that ejection of the nose during power-on flight could be accomplished safely. The flight of model A indicates that the three fins remaining on the model after collision with the wing were sufficient to damp out oscillations but the asymmetry after loss of one fin caused the model to follow a helical path. The accelerations during the flight indicate that escape might have been possible.

The flight of model B indicates that the separation phase of escape in this case would not have caused any great discomfort to a pilot. While an effort was made to make the ratio between the drag and weight of the nose and rear sections of the order of that of a full-scale airplane, this test represents an extreme case in that the aft body was stable after removal of the nose section. In the case of a conventional airplane, the aft fuselage after nose release would probably be unstable, and, because of this, its drag would be greatly increased.

The longitudinal acceleration-time curves shown in figure 9 indicate that the initial push given the nose section was necessary. When the two bodies were 4 to 5 inches apart, the shielding effect of the nose on the aft body caused the drag of the aft body to be so low that its deceleration was less than that of the nose. The initial added velocity given the nose section by the jettison charge was sufficient to widen the gap until the drag-weight ratios became favorable. Whether or not this would be true in the case of a full-scale airplane would depend upon the individual configuration of the airplane and nose section.

One factor that must be given consideration at high Mach numbers is the deceleration due to drag experienced after ejection. In figure 15 the instantaneous deceleration calculated for a 1500-pound nose section is plotted for three different altitudes using the RM-11 configuration but having linear dimensions five times those of the RM-11. In addition, the average decelerations experienced over a given elapsed time as computed from these instantaneous values are also presented for comparison with human-tolerance values. The line showing human tolerance is taken from unpublished data and is for a human body fully extended with the accelerations transverse to the human body. While the acceleration on the pilot in a jettisoned nose is applied in the same direction, some variation must be expected because of a pilot having his legs forward in a sitting position. The plot indicates that the deceleration due to drag is not serious at a Mach number of 2.0 at altitudes above 30,000 feet.

It has been found that nose fins produce a detrimental effect on the stability of a complete airplane. The problem of making retractable fins that are of sufficient stiffness, take up little space, and are still capable of being extended almost instantaneously is very great. One possible method of compromise might be to have the fins permanently attached but able to float freely. They could be locked in position of zero incidence quickly and with a fairly simple mechanism. By using this method the drag of the fins is present but it would probably eliminate the destabilizing effect. An investigation of the effect of such fins on stability and of susceptibility to flutter would be necessary.

Since the terminal velocity of most jettisoned nose sections would probably be too high for direct escape into the air stream, some means of slowing down the nose will probably be necessary. In view of the fact that it is desirable to keep any escape device as simple as possible, it might be desirable to use a drag parachute to decrease the terminal velocity rather than drag flaps.

CONCLUSIONS

Results obtained from tests of rocket-propelled models to test the jettisonable-nose method of pilot escape indicated the following:

- (1) If the nose section is released during power-on flight, there is danger of collision with the main body of the airplane.
- (2) With suitable stabilizing fins the nose section may be forcibly ejected at a Mach number of 0.87 during power-off stable flight without producing accelerations dangerous to a pilot.
- (3) The drag-weight ratio of such a nose section should be made sufficiently less than the drag-weight ratio of the main body so that collision of the two after ejection is impossible.
- (4) The shielding effect of the nose section on the main body is considerable, and forcible ejection seems necessary for smooth separation.

Calculations for the configuration tested indicated that the deceleration due to drag on the nose section after separation will not be dangerous to a pilot at Mach number 2.0 at altitudes above 30,000 feet.

Langley Aeronautical Laboratory
National Advisory Committee for Aeronautics
Langley Air Force Base, Va.

REFERENCES

1. Marzella, J., and Hess, J. R.: Ground and Flight Tests of Martin-Baker Aircraft Company Pilot's Ejection Seat from Model JD-1 Airplane. Rep. ASL NAM 256005.1, Part I, Naval Air Exp. Sta., Bur. Aero., Feb. 27, 1947.
2. Armstrong, Harry G., and Heim, J. W.: The Effect of Acceleration on the Living Organism. ACTR 4362, Materiel Div., Army Air Corps. Dec. 1, 1937.
3. Scher, Stanley H.: Wind-Tunnel Investigation of the Stability of Jettisoned Nose Sections of the D-558 Airplane - Phases I and II. NACA RM L7K10, 1948.
4. Angle, Ellwyn E.: Initial Flight Test of the NACA FR-1-A, a Low-Acceleration Rocket-Propelled Vehicle for Transonic Flutter Research. NACA RM L7J08, 1948.

~~CONFIDENTIAL~~

TABLE I

MASS-BALANCE CHARACTERISTICS OF MODELS

	Model A	Model B
Complete model:		
Weight at launching	253.3	252.5
Weight at burnout	187.9	187.1
C.G. location at launching, in. from tip of nose	54	54
C.G. location at burnout, in. from tip of nose	52.4	52.4
Jettisonable nose:		
Weight	42.4	41.44
C.G. location, in. from tip	24	24.5
Moment of inertia (roll axis), slug-ft ²	0.103	0.111
Moment of inertia (pitch axis), slug-ft ²	1.14	0.813
Moment of inertia (yaw axis), slug-ft ²	1.14	0.813

NACA

TABLE II

ACCELEROMETER POSITIONS IN JETTISONABLE NOSE OF RM-11 MODELS

[All figs. are in. from c.g.]

Accelerometer	Above c.g.	Beside c.g.	Behind c.g.
Model A			
Longitudinal	0.92	3.25	1.86
Normal	4.21	0	3.92
Transverse	2.1	2.57	3.92
Model B			
Longitudinal	-1.60	3.12	1.3
Normal	4.21	0	3.43
Transverse	2.1	2.57	3.43

NACA

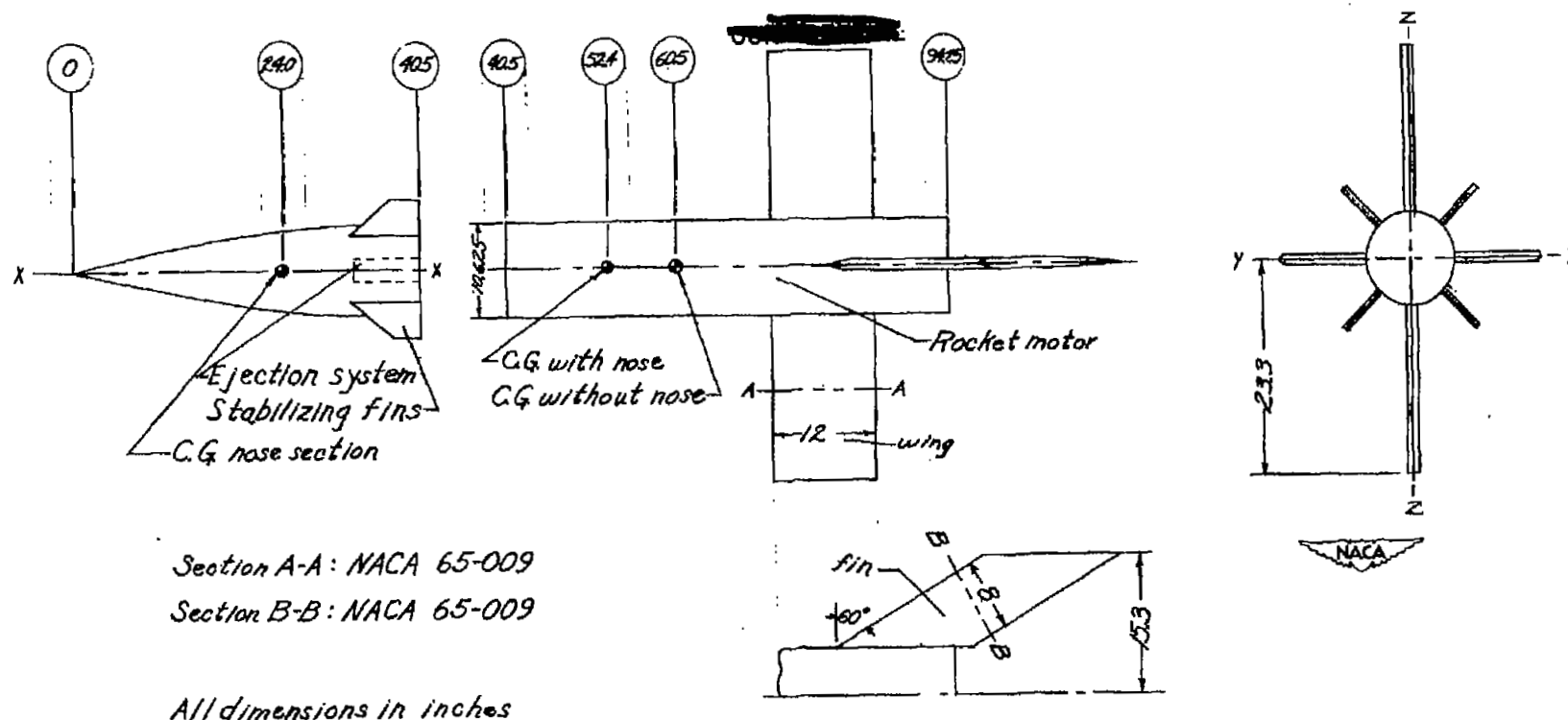


Figure 1.— Sketch of RM-11 pilot-escape test vehicle.

~~CONFIDENTIAL~~

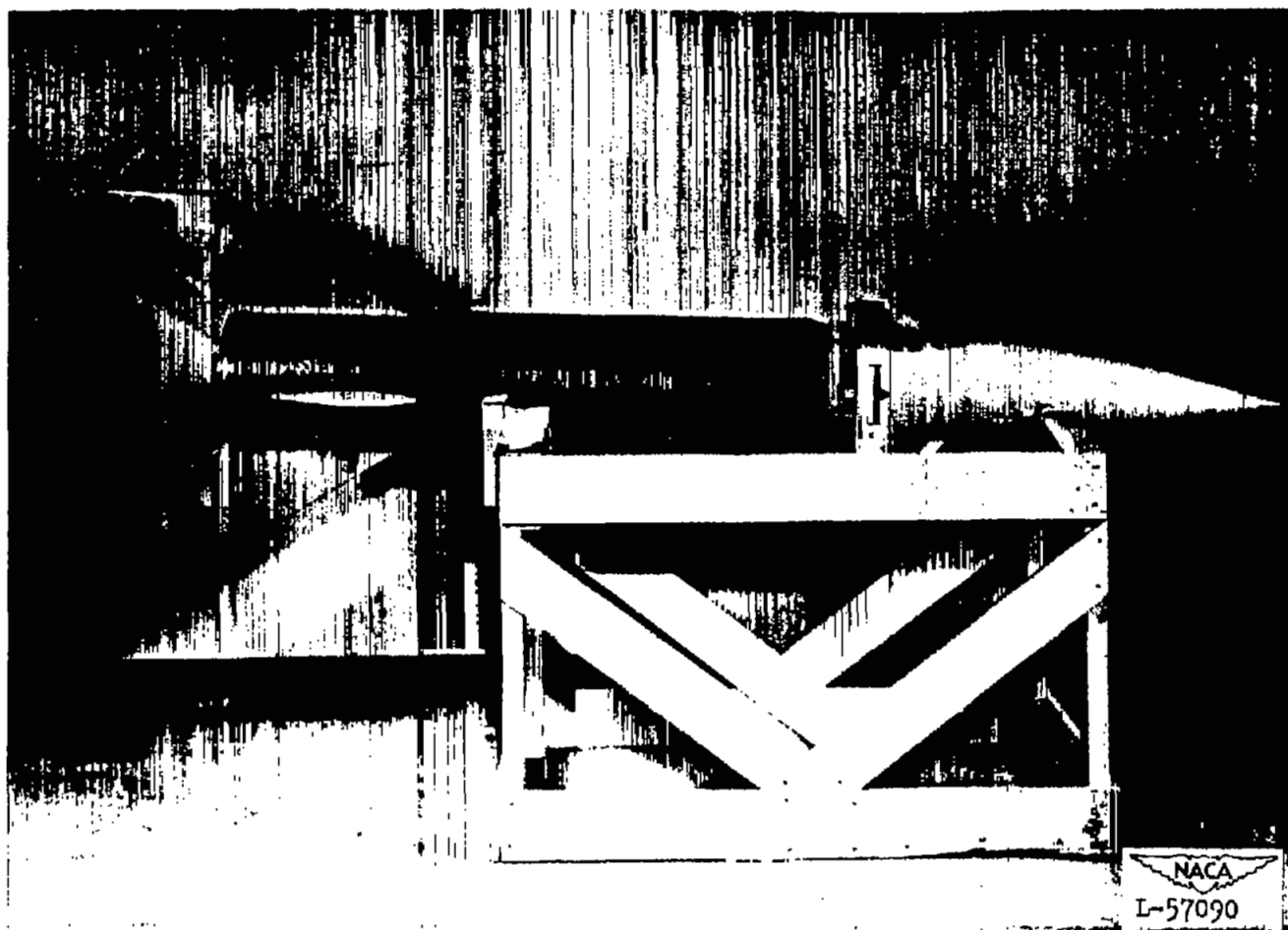


Figure 2.- RM-11 pilot-escape test vehicle.

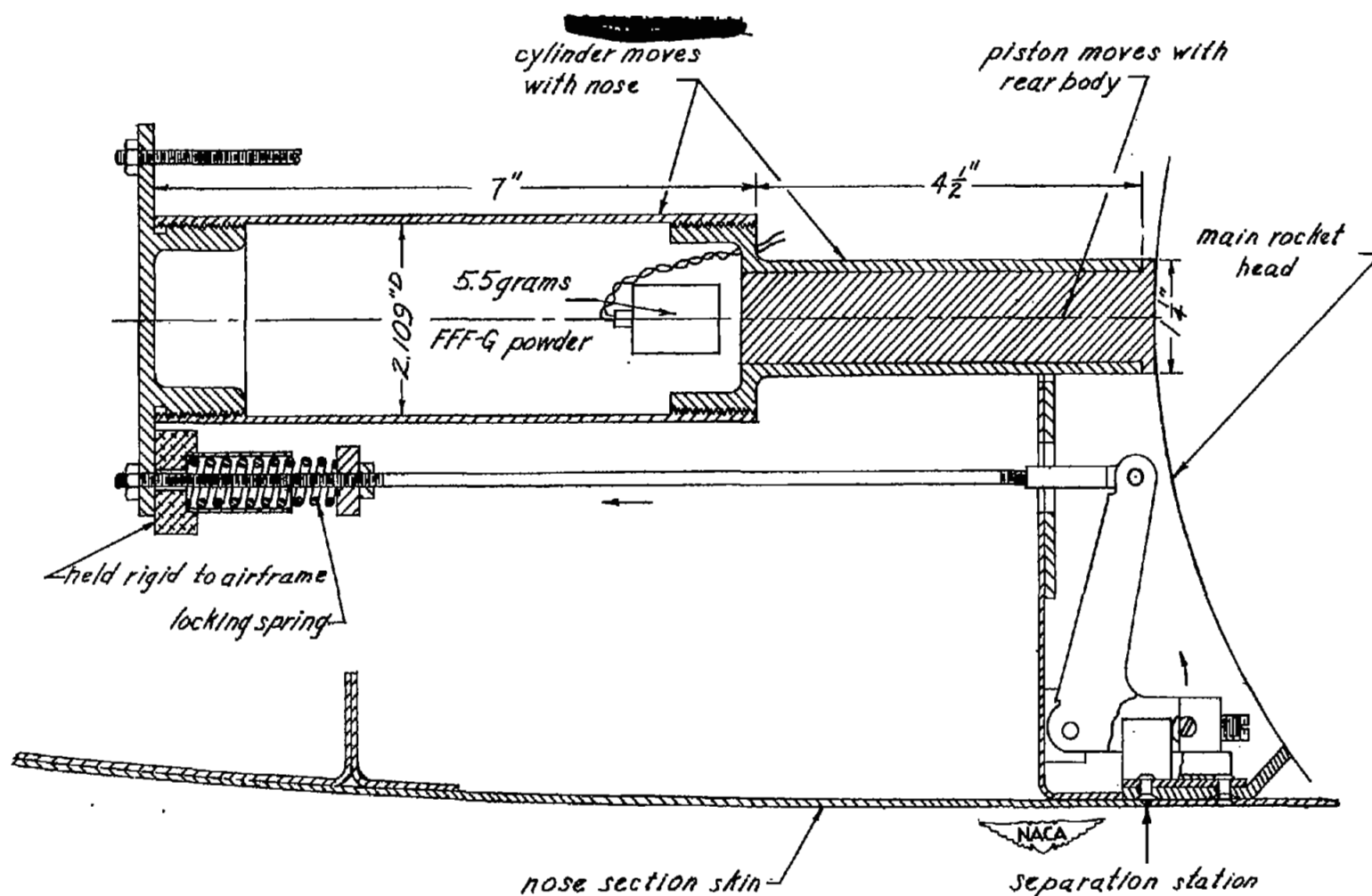


Figure 3.- RM-11 nose-section release mechanism.

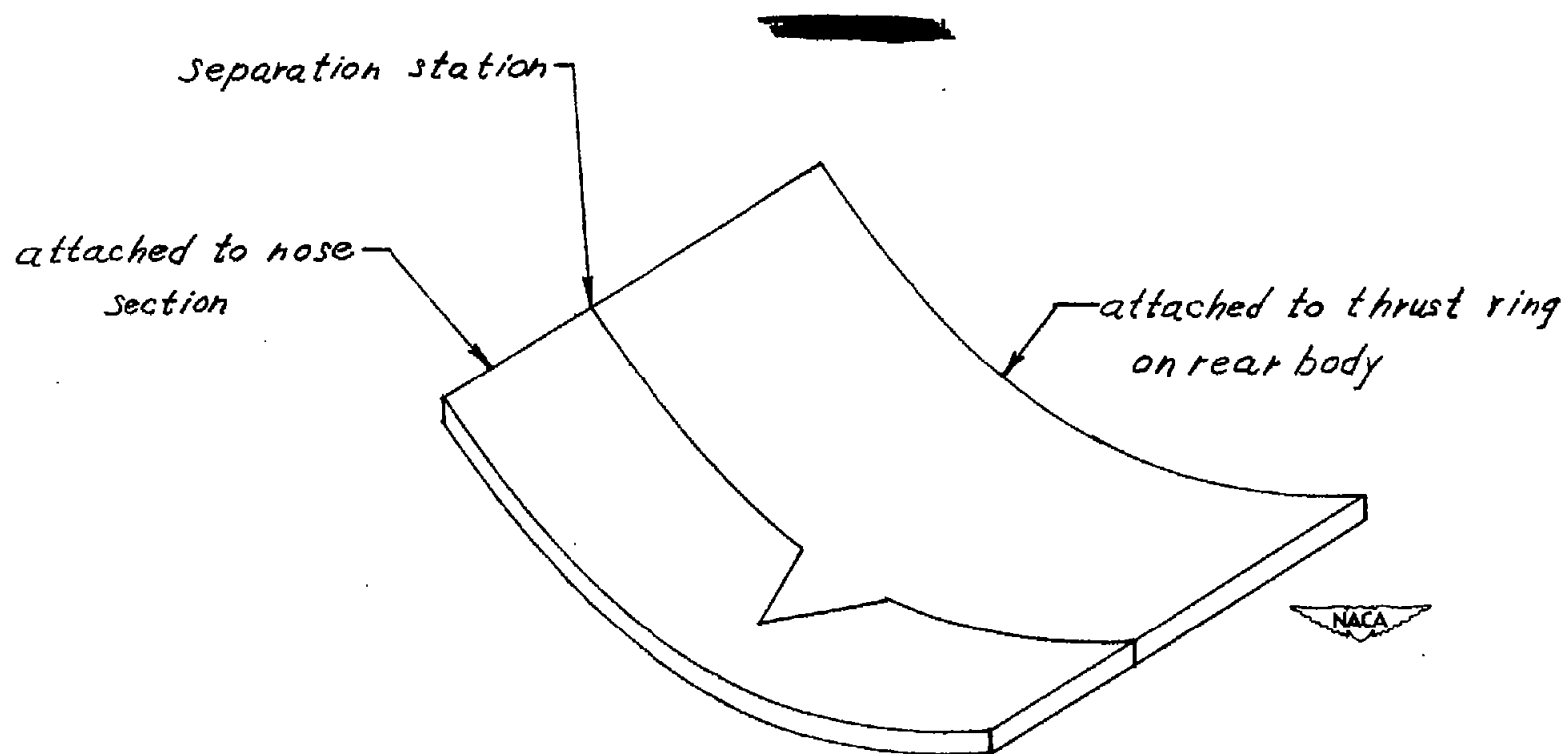


Figure 4.- Bearing plates.

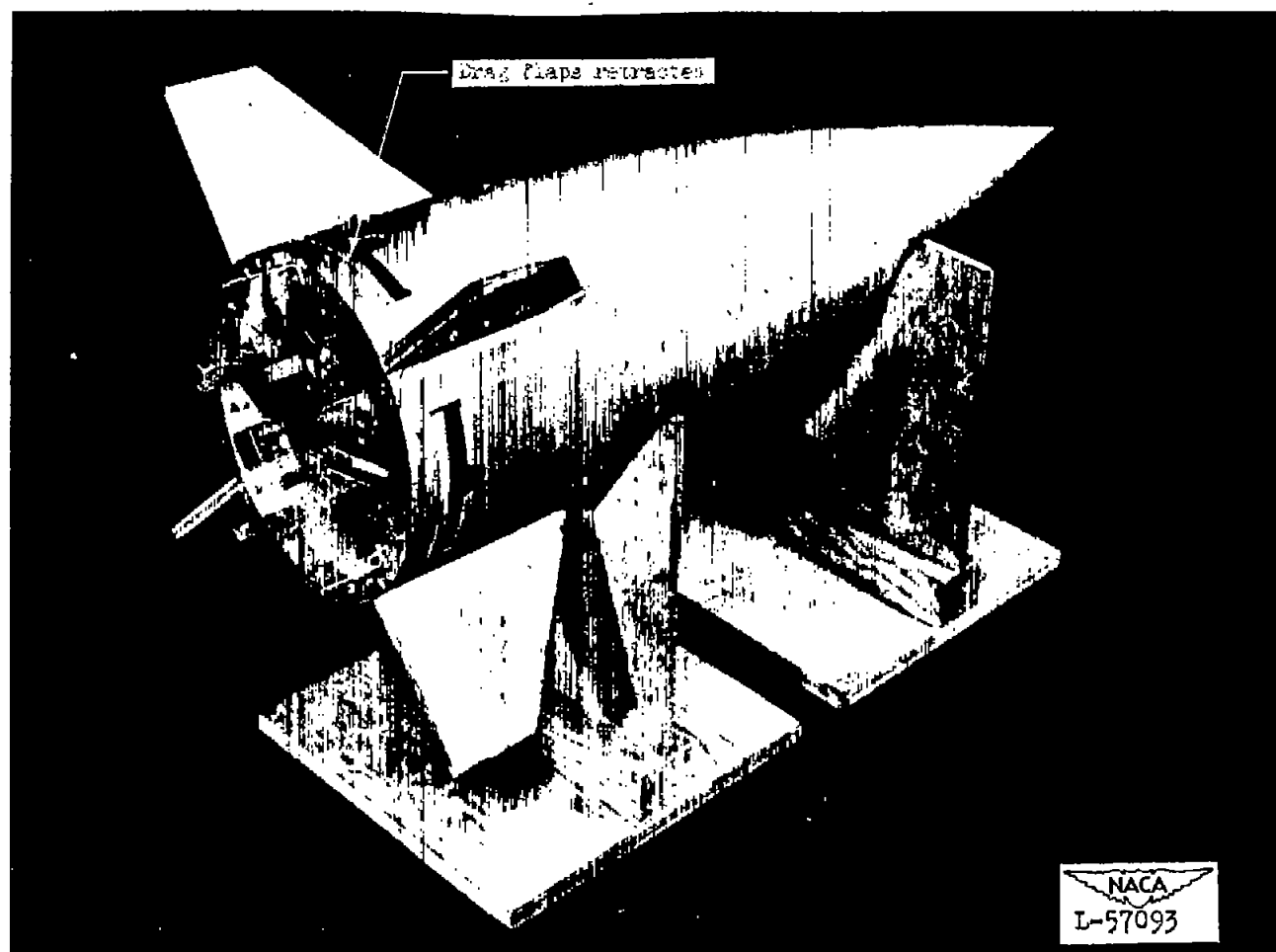


Figure 5.- RM-11 jettisonable nose. Flaps retracted.

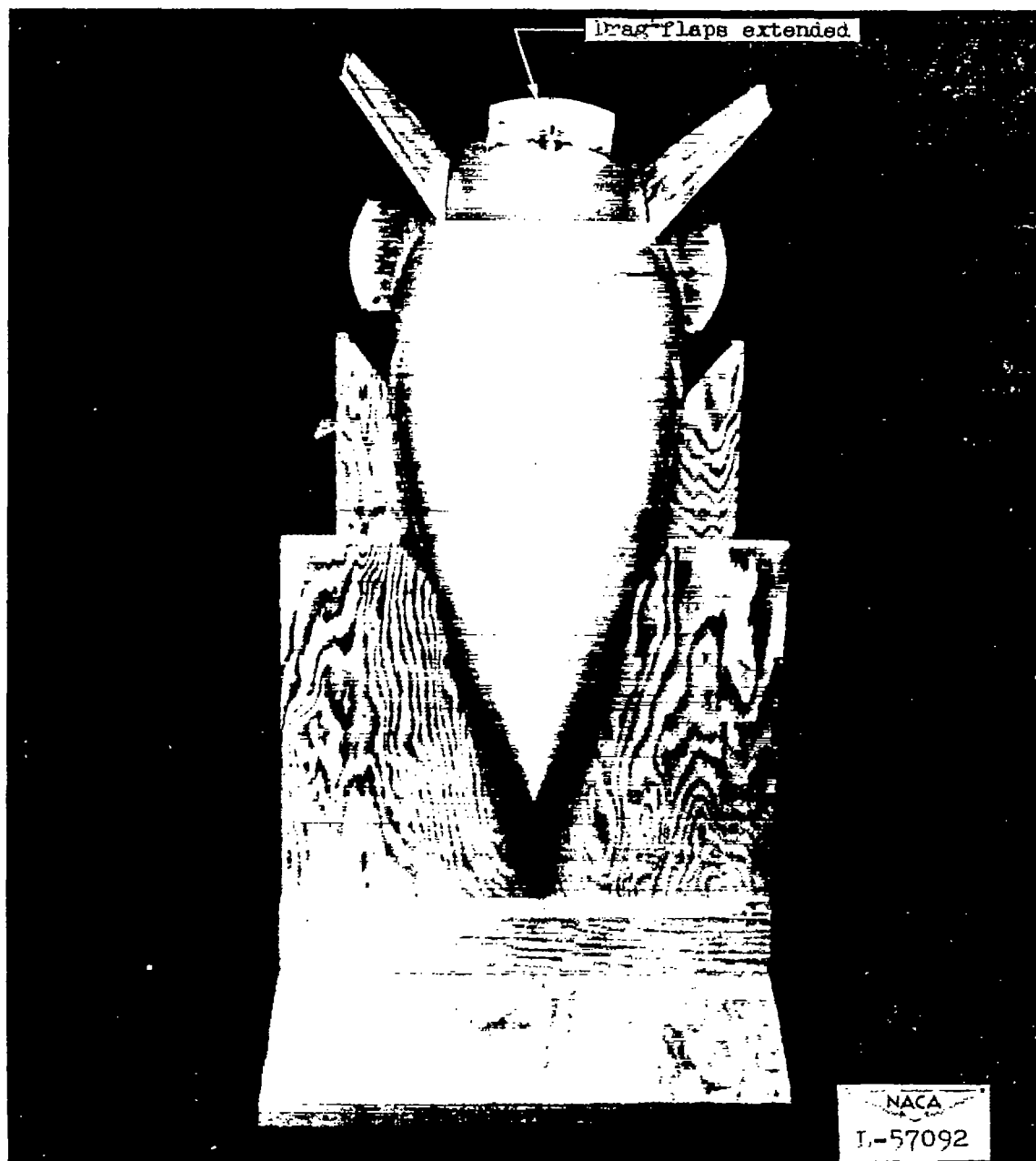


Figure 6.- RM-11 jettisonable nose. Flaps open.

15

16

17

18

19

20

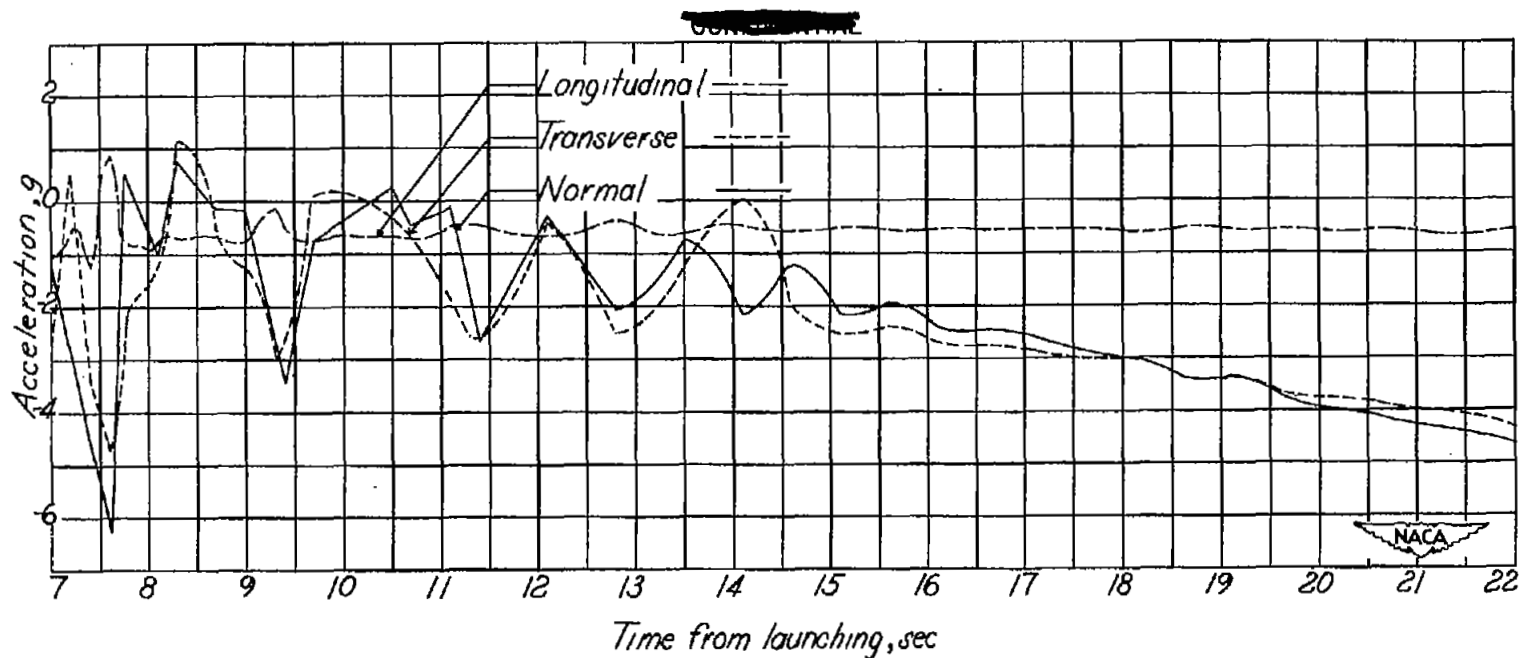


Figure 7.- Portion of accelerometer curves, RM-11A.

~~CONFIDENTIAL~~

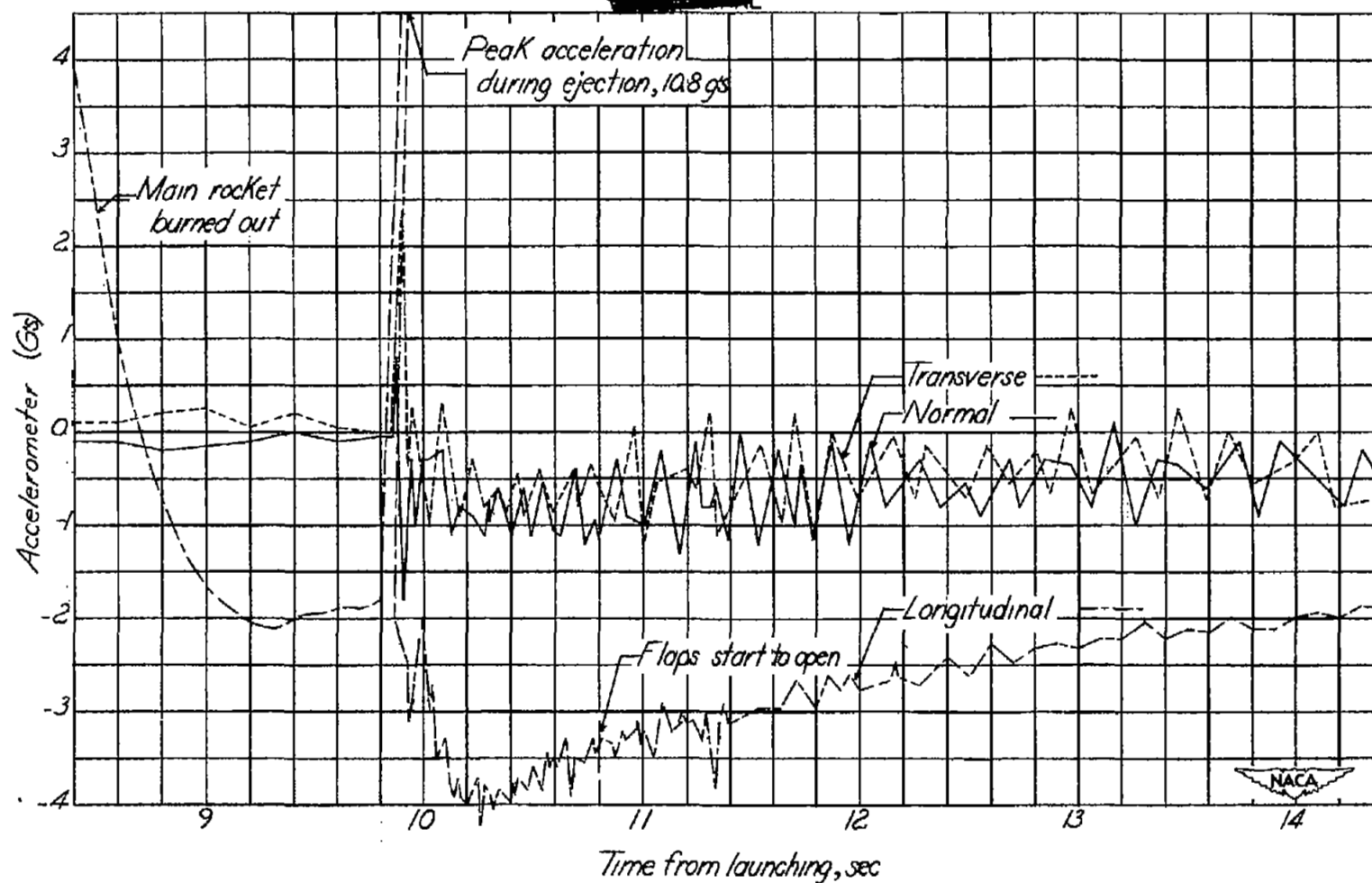


Figure 8.— Portion of accelerometer curves, RM-11B.

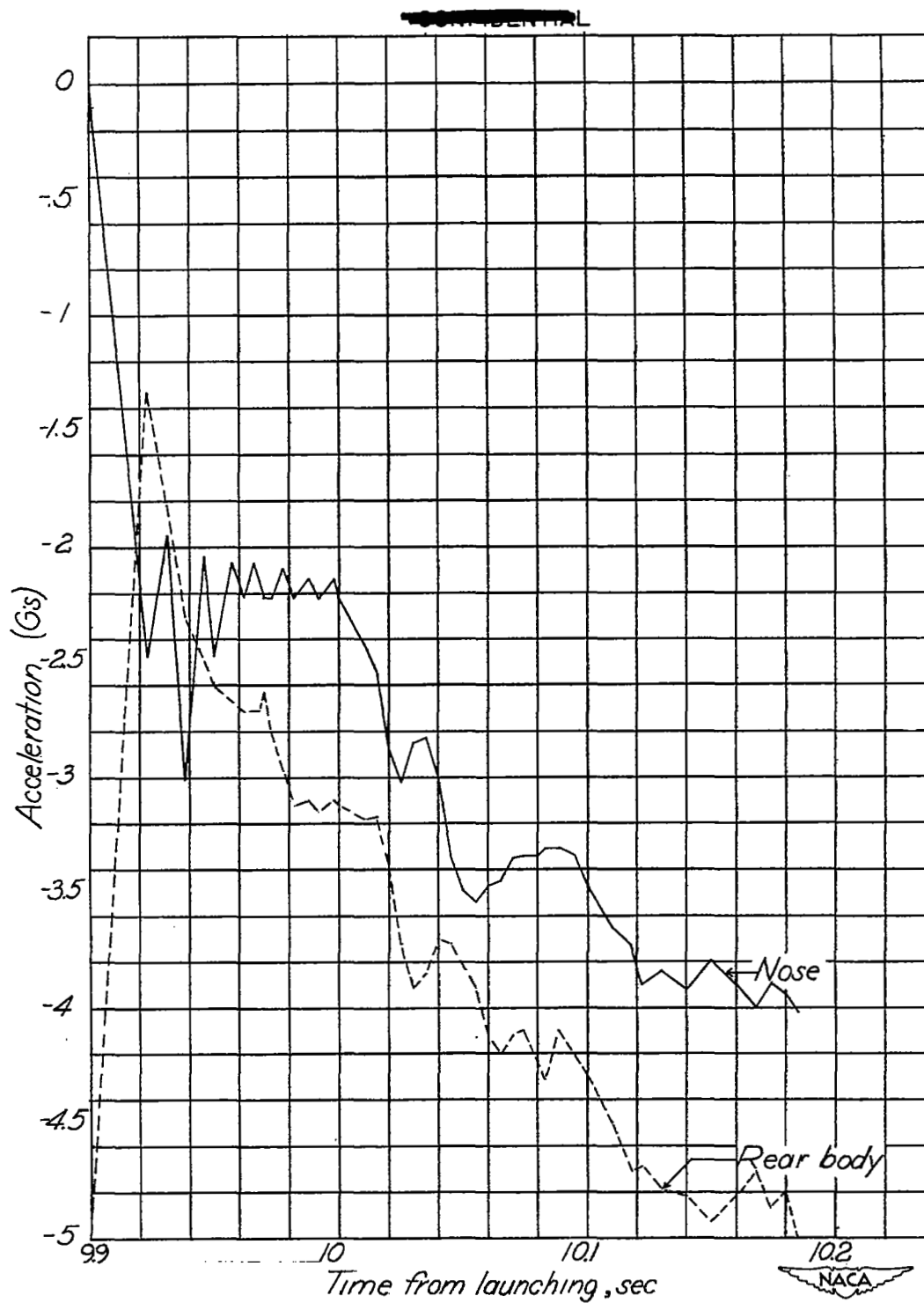


Figure 9.— RM-11B longitudinal acceleration of nose and rear body during separation.

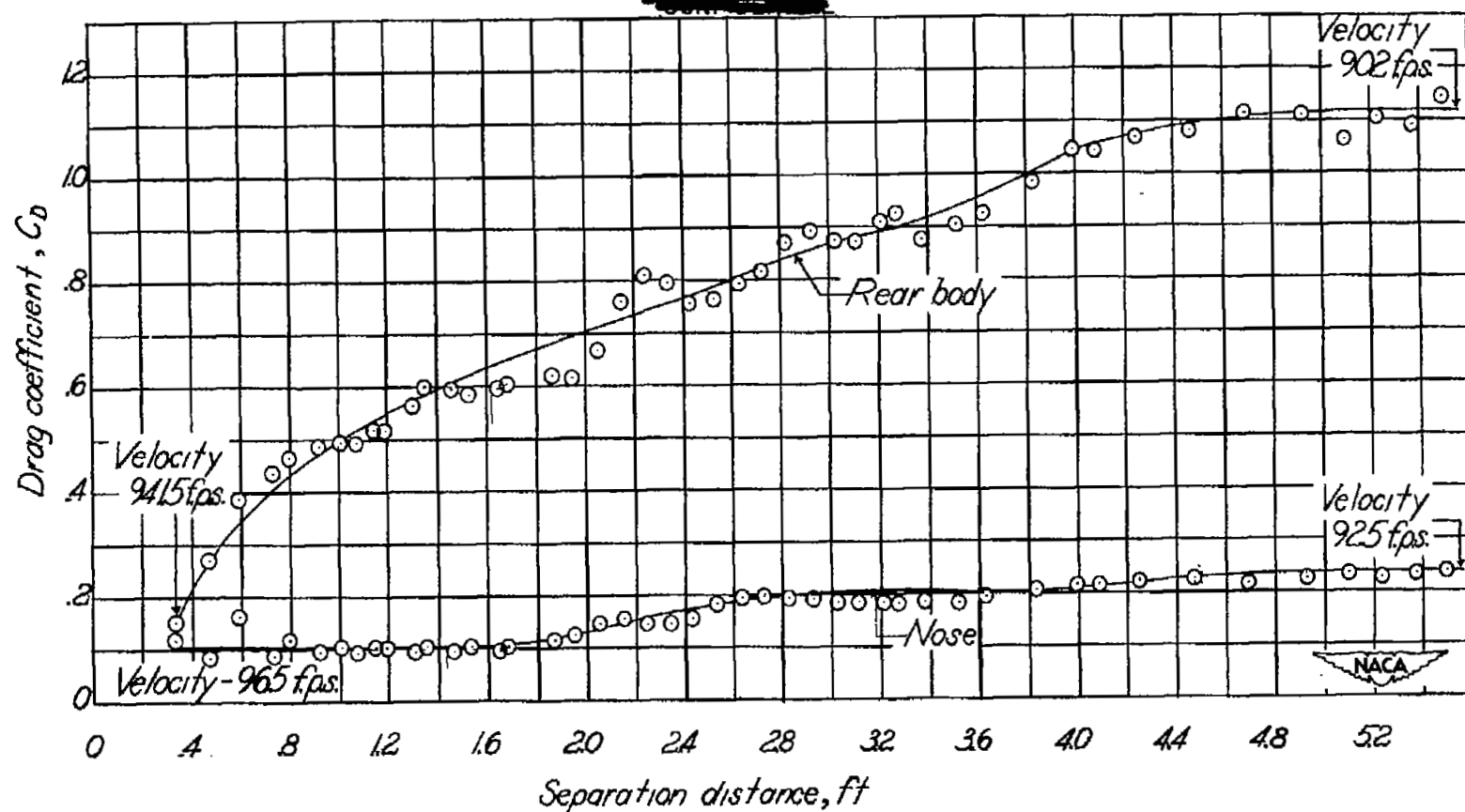


Figure 10.- RM-11B drag coefficient curves during separation.

~~CONFIDENTIAL~~

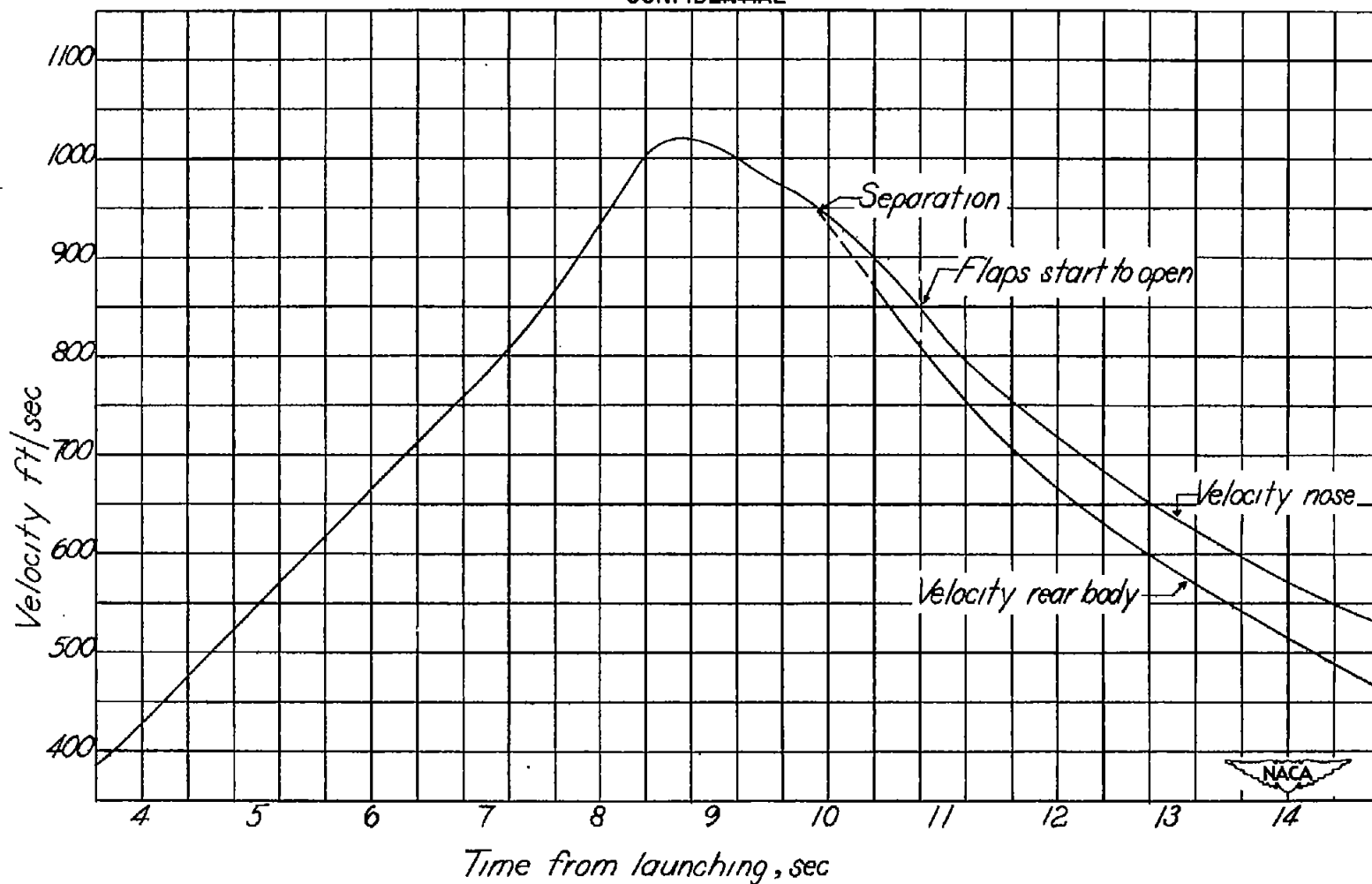


Figure 11.- RM-11B velocity plotted against time from Doppler radar.

~~CONFIDENTIAL~~

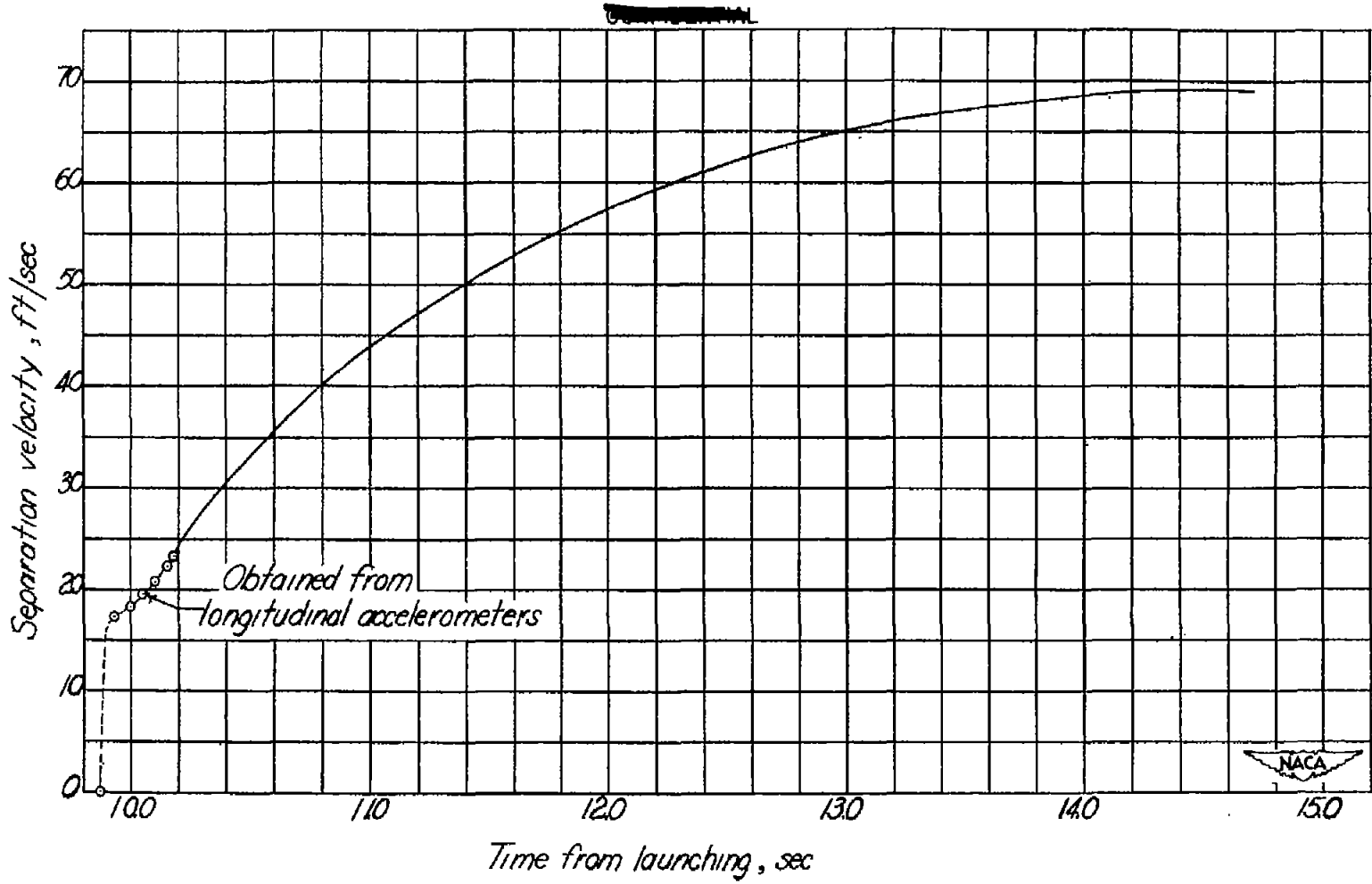


Figure 12.- Separation velocity plotted against time.

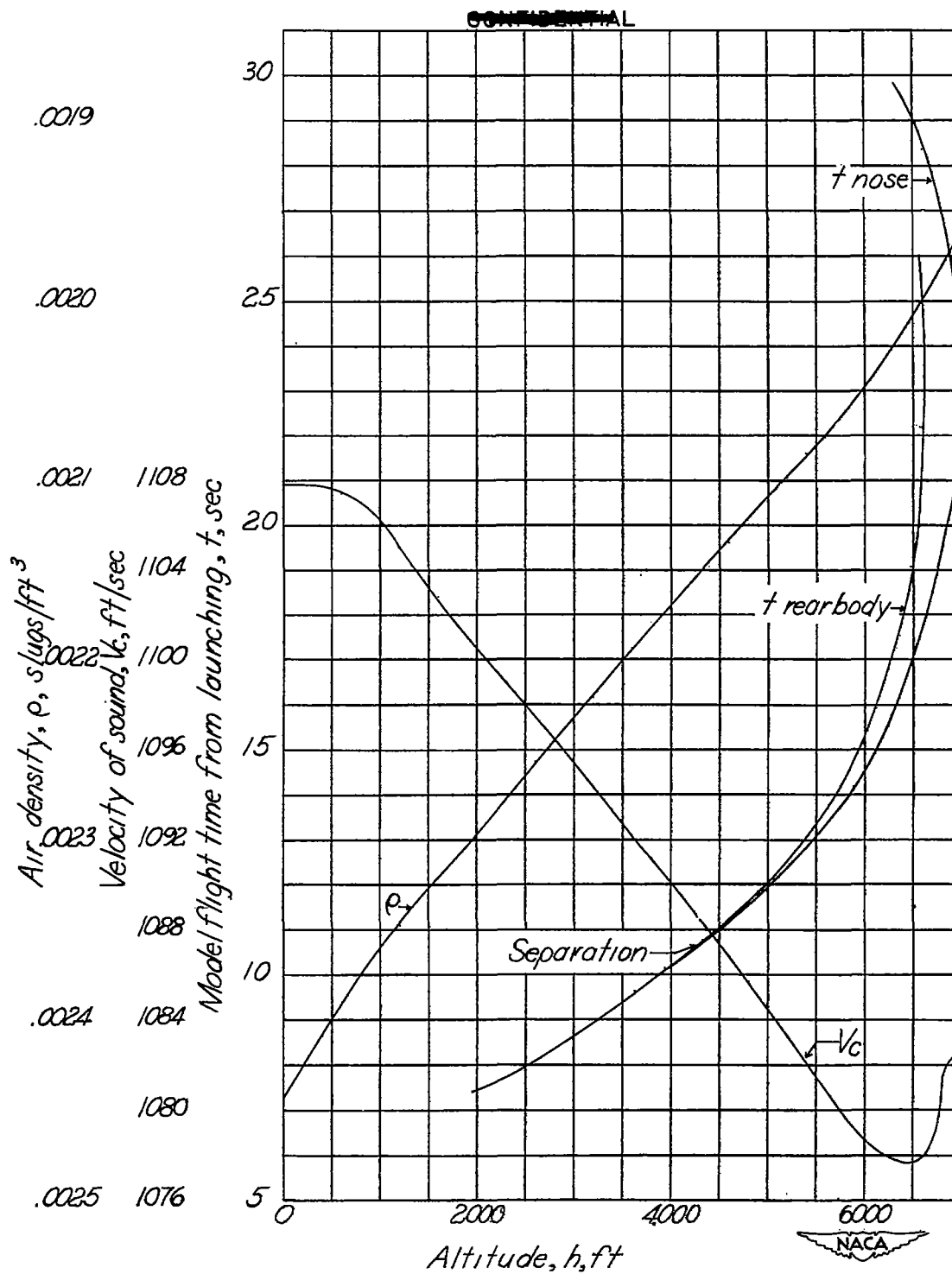


Figure 13.— Flight conditions of RM-11B.

~~CONFIDENTIAL~~

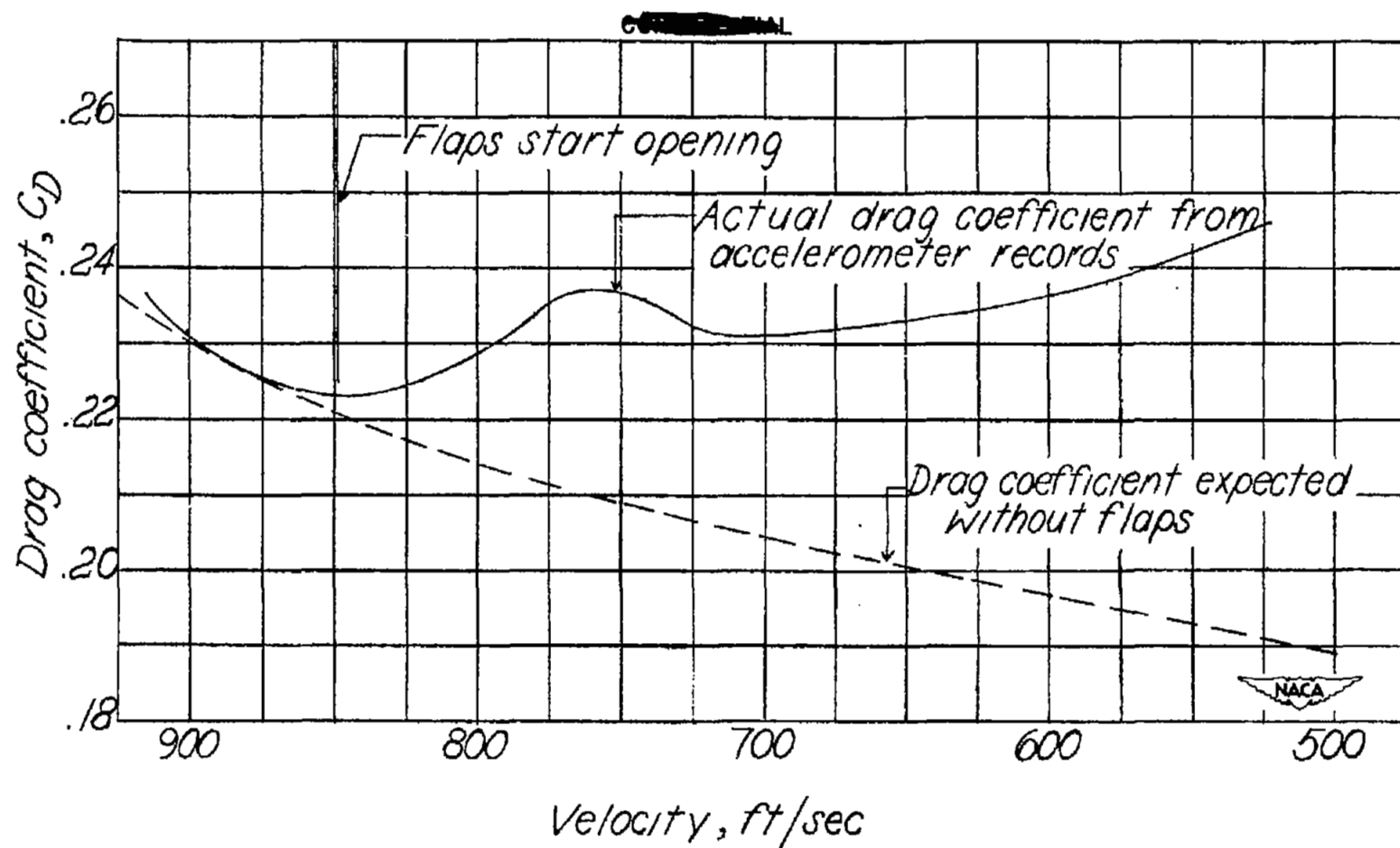


Figure 14.— RM-11B drag coefficient of nose section plotted against velocity.

~~CONFIDENTIAL~~

~~CONFIDENTIAL~~

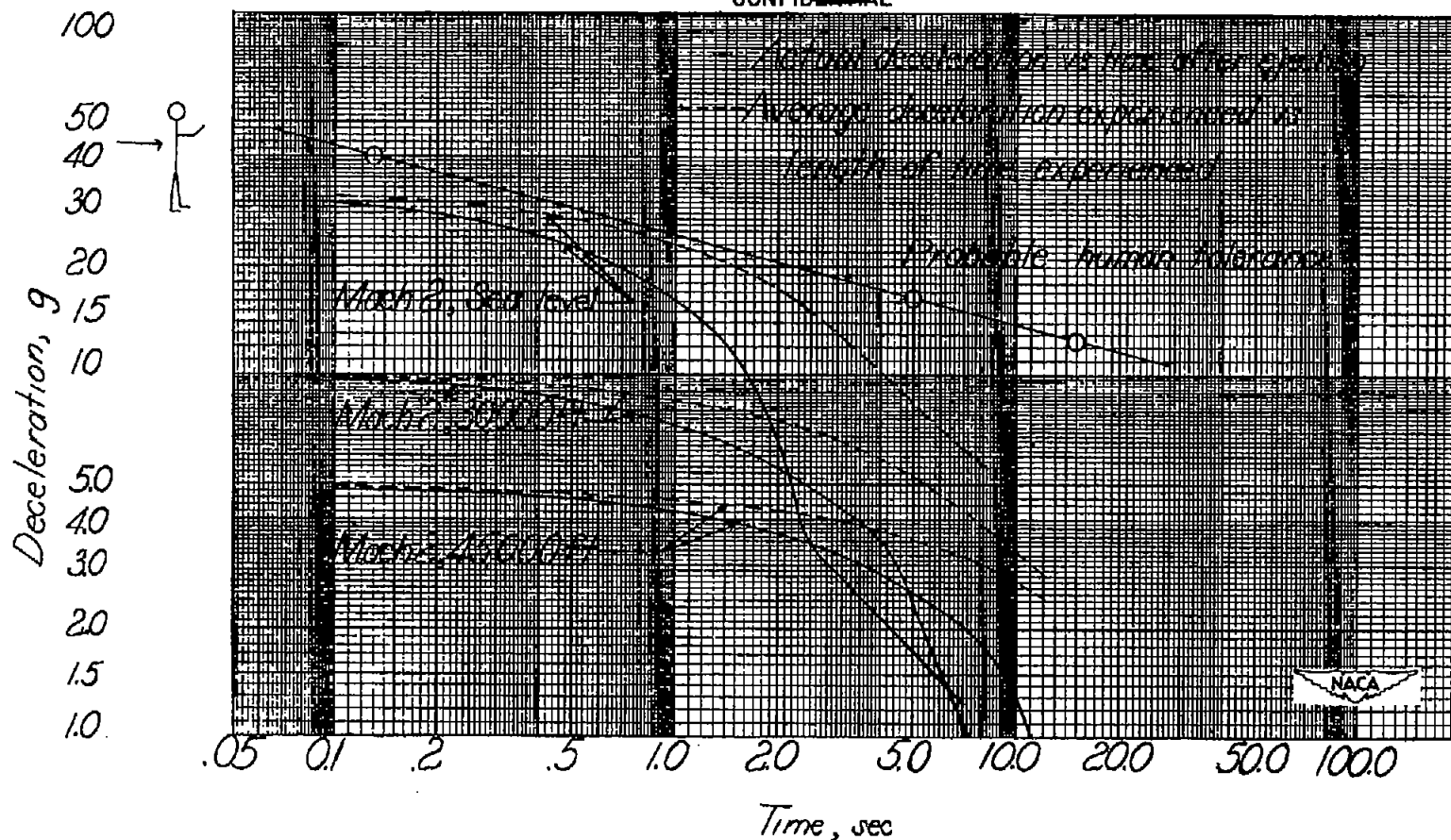


Figure 15.- Calculated decelerations due to drag of a 1500-pound nose jettisoned at various altitudes.

~~CONFIDENTIAL~~

NASA Technical Library



3 1176 01436 7321